ARMY RESEARCH LABORATORY

Quantifying Bulk Plasticity and Predicting Transition Velocities for Armor Ceramics Using Hardness Indentation Tests

by Corydon D. Hilton, James W. McCauley, Jeffrey J. Swab, Eugene R. Shanholtz, and Andrew R. Portune

ARL-TR-6050 **July 2012**

NOTICES

Disclaimers

The findings in this report are not to be construed as an official Department of the Army position unless so designated by other authorized documents.

Citation of manufacturer's or trade names does not constitute an official endorsement or approval of the use thereof.

Destroy this report when it is no longer needed. Do not return it to the originator.

Army Research Laboratory
Aberdeen Proving Ground, MD 21005-5069

ARL-TR-6050 **July 2012**

Quantifying Bulk Plasticity and Predicting Transition Velocities for Armor Ceramics Using Hardness Indentation Tests

James W. McCauley and Jeffrey J. Swab
Weapons and Materials Research Directorate, ARL

Corydon D. Hilton, Eugene R. Shanholtz, and Andrew R. Portune
Oak Ridge Institute for Science and Education

REPORT DOCUMENTATION PAGE	Form Approved OMB No. 0704-0188

1. REPORT DATE *(DD-MM-YYYY)*	2. REPORT TYPE	3. DATES COVERED (From - To)
July 2012	Final	October 2008–September 2011

4. TITLE AND SUBTITLE
Quantifying Bulk Plasticity and Predicting Transition Velocities for Armor Ceramics Using Hardness Indentation Tests

5a. CONTRACT NUMBER

5b. GRANT NUMBER

5c. PROGRAM ELEMENT NUMBER

6. AUTHOR(S)
Corydon D. Hilton,* James W. McCauley, Jeffrey J. Swab, Eugene R. Shanholtz,* and Andrew R. Portune*

5d. PROJECT NUMBER
AH42

5e. TASK NUMBER

5f. WORK UNIT NUMBER

7. PERFORMING ORGANIZATION NAME(S) AND ADDRESS(ES)
U.S. Army Research Laboratory
ATTN: RDRL-WMM-E
Aberdeen Proving Ground, MD 21005-5069

8. PERFORMING ORGANIZATION REPORT NUMBER
ARL-TR-6050

9. SPONSORING/MONITORING AGENCY NAME(S) AND ADDRESS(ES)

10. SPONSOR/MONITOR'S ACRONYM(S)

11. SPONSOR/MONITOR'S REPORT NUMBER(S)

12. DISTRIBUTION/AVAILABILITY STATEMENT
Approved for public release; distribution is unlimited.

13. SUPPLEMENTARY NOTES
*Oak Ridge Institute for Science and Education, Oak Ridge, TN 37831

14. ABSTRACT
Many studies have shown that harder ceramics generally perform better in armor applications; however, the nature of the relationship between hardness and ballistic performance is not understood to a degree that is useful in materials development. In addition, some research has suggested that a material's potential for inelastic deformation (or its "quasi-plasticity"—a bulk property) may also play an important role in its resistance to penetration. Methods of quantifying the bulk plasticity of a ceramic material are, however, extremely limited. Recently, an empirical approach has been described in which hardness tests are used to quantify bulk plasticity in structural ceramics and predict their transition velocities. The current study extends this approach to a wider variety of potential armor ceramics. For those ceramics that have been tested in dwell/penetration transition experiments, the transition velocities predicted by this approach generally show excellent agreement (within 5% in most cases) with the experimentally determined velocities. Furthermore, the robustness of the technique is demonstrated through the incorporation of multiple operators and multiple hardness-testing units.

15. SUBJECT TERMS
plasticity, hardness, indentation, ceramic armor, transition velocity

16. SECURITY CLASSIFICATION OF:			17. LIMITATION OF ABSTRACT	18. NUMBER OF PAGES	19a. NAME OF RESPONSIBLE PERSON
a. REPORT	b. ABSTRACT	c. THIS PAGE			Corydon D. Hilton
Unclassified	Unclassified	Unclassified	UU	32	19b. TELEPHONE NUMBER (*Include area code*) 410-306-0753

Standard Form 298 (Rev. 8/98)
Prescribed by ANSI Std. Z39.18

Contents

List of Figures

List of Tables

Acknowledgments

The assistance of Dominic Danna with hardness testing is gratefully appreciated.

This research was supported in part by appointments to the Internship and Postgraduate Research Participation Programs at the U.S. Army Research Laboratory (ARL), administered by the Oak Ridge Institute for Science and Education through an interagency agreement between the U.S. Department of Energy and ARL.

1. Introduction

Many studies have shown that hardness is a very important property for ceramics used in armor applications (*1–7*). In general, armor ceramics should be harder than the penetrator material. Sufficient hardness allows the ceramic to fracture, fragment, and/or deform the impacting projectile. Viechnicki et al. (*1*) measured V50 values in experiments where ceramic plates (TiB_2, SiC, and Al_2O_3) were impacted with 97 weight-percent tungsten long-rod penetrators. The authors compared ballistic performance with a variety of static mechanical properties and concluded that hardness is the only single property that may be used to help predict ballistic performance. Flinders et al. (*2*) performed ballistic tests on multiple SiC-based ceramic materials using WC-Co cored projectiles and found that depth of penetration (DOP) values correlated very well with Knoop hardness measurements. Krell and Strassburger (*3*) investigated the impact performance of ultrafine grain α-Al_2O_3 in a DOP test configuration using a tungsten-alloy penetrator material, and observed a linear relationship between ballistic mass efficiency and Vickers hardness. Although it has been well documented that a relation exists between hardness and the ballistic performance of advanced ceramics, the relationship is not understood well enough to be useful in guiding the development of new, improved armor materials.

Some studies have suggested that the ability of a ceramic material to deform inelastically (or its "quasi-plasticity") may also play an important role in its ballistic response (*7*, *8*). In ballistic applications, quasi-plasticity reduces the magnitude of local stresses and spreads the applied load over a larger volume of material. It may also suppress the formation of catastrophic macrocracks. The role of plastic deformation in the impact response of ceramics was first investigated over four decades ago by Wilkins et al. (*9*). It was observed that in ballistic tests involving hard-steel-core small-arm projectiles, BeO's ability to deform plastically allowed it to resist failure for a longer time than other, more brittle materials. This led the authors to explore methods for introducing "ductility" into ceramics. Magnusson and Shen (*10*) state that "to really improve the protection performance, ceramic materials that allow some amount of inelastic deformation (plasticity) are desired." The authors proposed that the formation of nanograin microstructures may allow such improvements, and results of their study indeed revealed improvements in the ballistic performance of nanograin Si_3N_4 relative to micrograin Si_3N_4.

2. Background

2.1 Quantifying Quasi-Plasticity in Ceramics

While methods of determining the hardness values of ceramic materials have been established and standardized for a number of years, there are no widely-accepted techniques for quantifying plasticity in these materials. In general, ceramics are brittle materials that are unable to accommodate significant macroscopic plastic strains. However, examination of indent sites and/or indentation stress-strain behavior in several ceramic materials has shown that they may experience inelastic deformation mechanisms, such as microcracking, microcleavage, slip, and twinning, at room temperature (*7*, *11–17*). This has led some researchers to propose the use of indentation techniques as a means of "quantifying" quasi-plastic deformation in these materials. Milman (*18*) developed a plasticity characteristic that is defined by the ratio of the plastic strain to the total elastoplastic strain experienced by a material during a hardness indentation event. The characteristic has been applied to brittle ceramics as well as ductile metals. Lawn and others (*19–22*) describe similar expressions that can be used as elasticity-plasticity parameters to classify ceramics and glasses. These expressions are also based on the deformations that occur in a material during an indentation cycle, and they compare the impression depth after unloading to the maximum depth achieved during the loading process. It should be noted that each of these elasticity-plasticity expressions greatly depends on the ratio of hardness to modulus (H/E). In fact, McColm (*20*) suggested the use of H/E as a "plasticity parameter" and has compared values of this ratio for various materials. A new hardness-based approach to quantifying bulk plasticity in ceramic materials, recently proposed by Wilantewicz and McCauley (*23*), will now be discussed.

In standard Knoop or Vickers tests, the hardness of ceramics generally decreases with increasing indentation load or indentation size—a behavior known as the indentation size effect (ISE) (*24–27*). McCauley and Wilantewicz (*28*) propose the existence of three main regions in hardness-load curves for these materials (figure 1): (1) a "low-load" region where elastic deformation dominates, (2) an intermediate region that is dominated by plastic deformation, and (3) a "high-load" region where extensive permanent damage/fracture tends to occur. The authors further suggest that the exponent of a power law function, which is fit to a material's Knoop hardness-load curve, can be used to indicate the amount of inelastic deformation that the material may experience during impact. This exponent can be represented as the slope of a line if the power law equation is rewritten in log-log form. Specifically, focus is placed on the slope of the line between 2.94 and 19.6 N (0.3 and 2 kg); it is assumed that these are the approximate bounds for the intermediate region, where the behavior of the curve is controlled by the plasticity of the material.

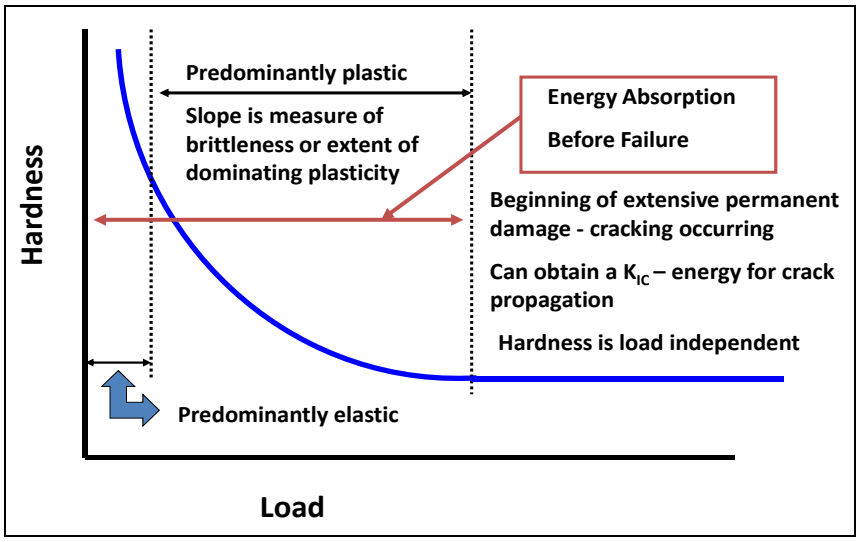

Figure 1. Knoop hardness-load curve of a typical ceramic illustrating three main deformation regimes.

The hardness-load curve in this "predominantly plastic" region can be described by the following power law equation:

$$HK=kF^{c}, \tag{1}$$

where HK is the Knoop hardness (N/m^2), F is the indentation load (N), and the k and c values are determined by a computer regression analysis; c is dimensionless, while k has the units $N^{(1-c)}/m^2$. (It should be noted that this expression is based on Meyer's law [*29*]). The exponent of the power-law equation, c, is indicative of how fast the Knoop hardness changes with change in the indentation load. It has a negative value because the Knoop hardness of ceramics decreases with increasing indentation load. Slopes for different ceramics can be easily compared if the power law relationship (equation 1) is rewritten in linear form, by taking the $\log_{10}$ of each side:

$$\log_{10} HK = \log_{10} k + c \log_{10} F . \tag{2}$$

A plot of $\log_{10}HK$ vs. $\log_{10}F$ will create a straight line with a slope c. Materials that are more brittle (those that are less capable of accommodating plastic strains) will tend to have steeper slopes. The magnitude of the ISE in these materials will be greater than in those materials that may have a greater tendency for inelastic deformation. (It should be mentioned that strong correlation has been shown between the scale of the ISE in ceramics and the H/E ratio [*30*].) It is therefore proposed that the absolute value of the reciprocal of the slope (c) is a semiquantitative measure of a ceramic material's bulk plasticity. Unlike previous approaches, where the amount of plasticity was determined at a single indentation load, this approach determines the plasticity from hardness measurements taken over a range of loads. During an impact event, materials with higher absolute, reciprocal c values will experience more quasi-plastic deformation.

2.2 Transition Velocity (TV)

Dwell is the phenomenon that occurs when a ceramic target is able to resist penetration by an impacting projectile, causing the projectile to flow radially outward along its surface. The "defeat" of a projectile in this manner, on the surface of the ceramic material, is called interface defeat. Hauver et al. (*31*) were the first to report on this phenomenon for long-rod projectiles. Interface defeat occurs when the impact pressure created by the impacting projectile is insufficient for penetration of the target. As the velocity of the projectile is increased, however, the critical impact pressure may be exceeded, and penetration of the ceramic target may take place. In general, this critical impact pressure does not exist as one particular pressure but actually corresponds to a range of pressures within which penetration may or may not occur. This range may be the result of slight material property variations. These critical pressures correspond to critical impact velocities, or transition velocities (TVs),* as they represent the transition from dwell to penetration of the target.

Lundberg et al. (*8*) conducted experimental and theoretical investigations on TVs of various ceramic materials. The impact experiments were performed using the reverse impact technique, where confined ceramic cylinders were launched into stationary projectiles. Several ceramic target materials were investigated (including SiC and TiB_2). Sintered tungsten alloy and molybdenum were used for projectile materials. Figure 2 shows flash x-ray images from these reverse impact experiments. The image on the left corresponds to an impact below the TV, while the image on the right is representative of impact above the TV (*32*). Based on compressive yield strengths (as estimated from hardness values) of the target materials, the authors developed models that were used to estimate lower and upper bounds for TVs (figure 3). The lower bound was based on the load distribution for a low-velocity water jet in combination with Boussinesq's elastic stress field solution for a point load on a semi-infinite elastic half space. The upper bound was estimated from a plastic slip-line solution for the indentation of a rigid punch. Lundberg's work suggests that compressive yield strength and quasi-plasticity are two factors that can significantly affect the impact resistance (TV) of a ceramic material.

*The TV values discussed in this study correspond to the experimental setup used by Lundberg et al. (*8*) and Lundberg and Lundberg (*33*) in their reverse impact experiments with tungsten heavy alloy (WHA) projectiles. These values greatly depend on the test conditions (projectile material, target confinement, projectile/target geometry, etc.) and should not be considered as unique material properties for the ceramics investigated, as changes in test conditions will likely lead to changes in TV values.

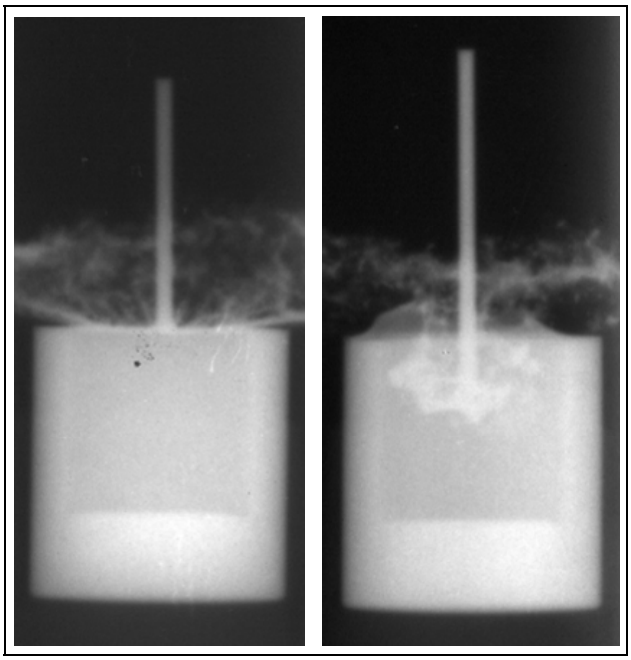

Figure 2. X-ray images showing interface defeat (left) and penetration (right) (*32*).

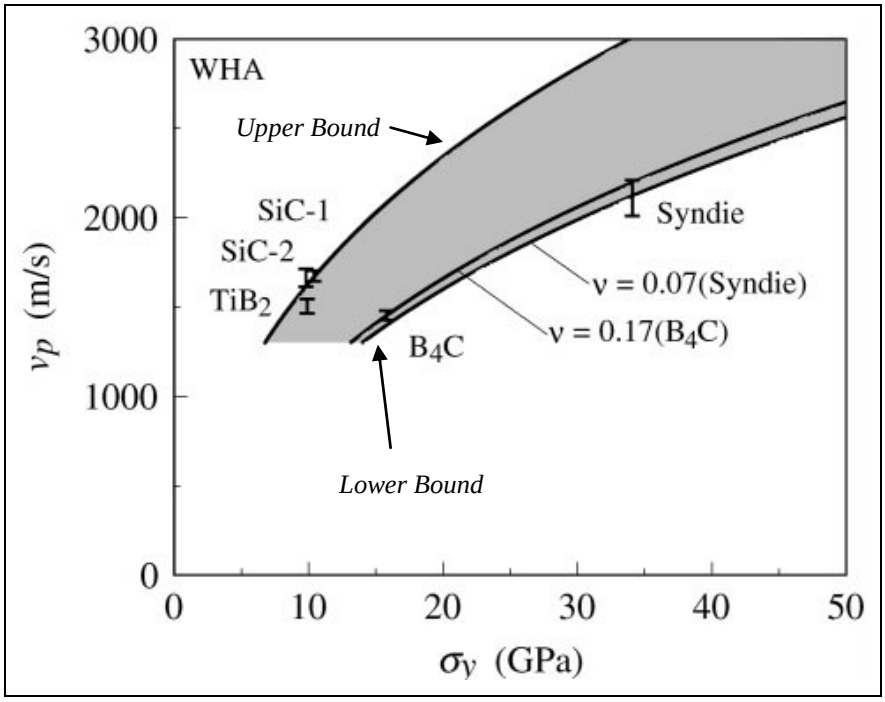

Figure 3. Bounds for transition velocity as a function of target compressive yield strength (*8*).

2.3 Transition Velocity Predictions by McCauley and Wilantewicz

McCauley and Wilantewicz (*28*) used the aforementioned approach (i.e., using absolute, reciprocal c value from the power law fit to Knoop hardness-load data) to estimate bulk plasticity values for various hot-pressed SiC materials manufactured by British Aerospace (BAE) Advanced Ceramics (formerly Cercom, currently CoorsTek). The plasticity of each ceramic was then combined with its hardness (at 1 N—this hardness value was obtained by extrapolating the power law fit to this load)* to obtain a quantitative parameter that represents "hardness + plasticity." Comparing this parameter with experimental TVs obtained by Lundberg and Lundberg (*33*) suggested a linear relationship between the two quantities (figure 4).

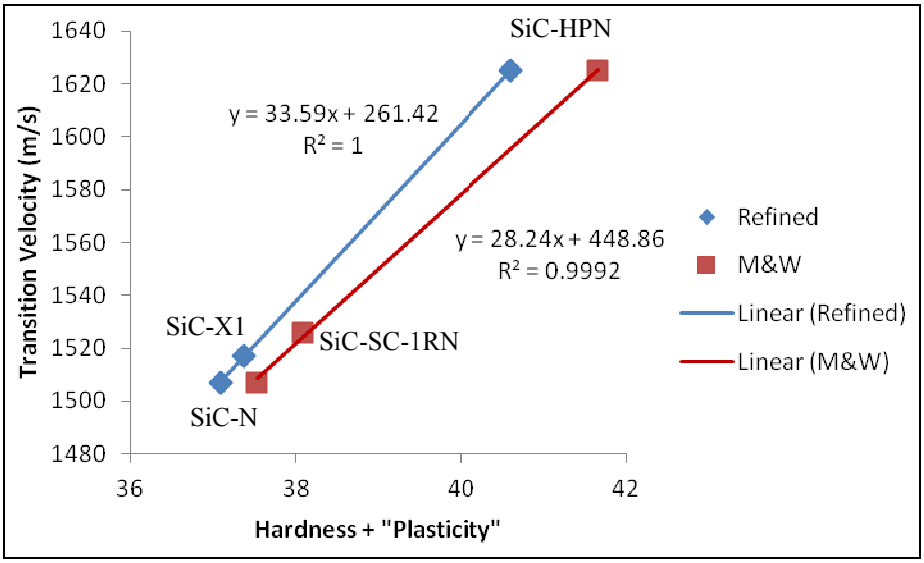

Figure 4. Experimentally measured transition velocities for SiC materials vs. "hardness + plasticity." Linear correlations were observed in the original analyses by McCauley and Wilantewicz (*28*) as well as an additional investigation by Hilton et al. (*34*).

A least-squares analysis of the data resulted in the following empirical relationship for determining TV of these ceramics:

$$TV = 28.24\,[\text{Hardness (1N)} + \text{Abs (1/c)}] + 448.86\,. \qquad (3)$$

The current investigation extends the original work of McCauley and Wilantewicz (*28*) and an investigation by Hilton et al. (*34*) to additional materials, and assesses the robustness of the predictive technique by incorporating multiple operators and hardness testing units.

*Extrapolation of the power law equation was used to obtain the HK values at 1 N. The indents created at this load are small in these hard materials, making accurate measurement of the diagonal lengths difficult and highly dependent upon the resolution of the images (or optics) used. Even minimal differences in diagonal length measurements can lead to large differences in measured HK values when examining very small indents.

3. Materials and Testing Procedures

Knoop indentation tests were performed at loads of 2.94, 4.9, 9.8, and 19.6 N on a variety of ceramics that are of interest for protection technologies. These included commonly used, opaque armor materials, such as Al_2O_3, B_4C, and SiC, as well as transparent armor materials Spinel and AlON, among others. In addition, two glasses (SLS Starfire and BS Borofloat) were investigated. Tests were performed by four operators (with varying levels of experience) using three different hardness testing units. Involving multiple operators and multiple hardness testing units allowed an assessment of the robustness of this hardness-based approach. As the test standard for Knoop indentation of advanced ceramics (*35*) states, the long slender tip of Knoop indents can be "difficult to discern, especially in materials with low contrast." Lighting intensity and field setting can also affect the apparent locations of the indent tips. Therefore, agreement in hardness results depends upon consistent, careful measurements by the operator, as well as the repeatability of the hardness tester. Each set of hardness-load data was fit to a power law equation (equation 1) to determine the exponent "c" and estimate the bulk plasticity value (Abs. [1/c]). The Knoop hardness at 1 N, "HK (1N)," was also determined from the power law fit. The plasticity value and the HK (1N) value were then combined and used in the "Refined" empirical equation (shown in figure 4 and discussed in section 4) to predict a TV for each material. Comparisons between predicted TV values and measured TV values were made for those materials that have been tested experimentally.

4. Results and Discussion

Typical hardness-load curves for four of the materials investigated in the current study are shown in figure 5. As previously mentioned, HK values were obtained at four indentation loads for each material. The R^2 (the square of the correlation coefficient for the power-law fit) values indicate that the power-law equation tends to fit the hardness-load data very well, as all values are above 0.96.

4.1 Refinement and Applicability of the Approach

Equation 3 was generated by McCauley and Wilantewicz (*28*) based on hardness data for SiC-N, SiC-HPN, and SiC-SC-1RN. Using this equation along with hardness data that has been generated for SiC-X1 and AlON, predicted TV values between 1474 and 1530 m/s have been obtained for SiC-X1, while TV values between 1232 and 1278 m/s have been predicted for AlON. All predicted velocities are within 3% of the mean measured TV (1517 m/s) for SiC-X1 and within 14% of the respective value for AlON (1217 m/s).

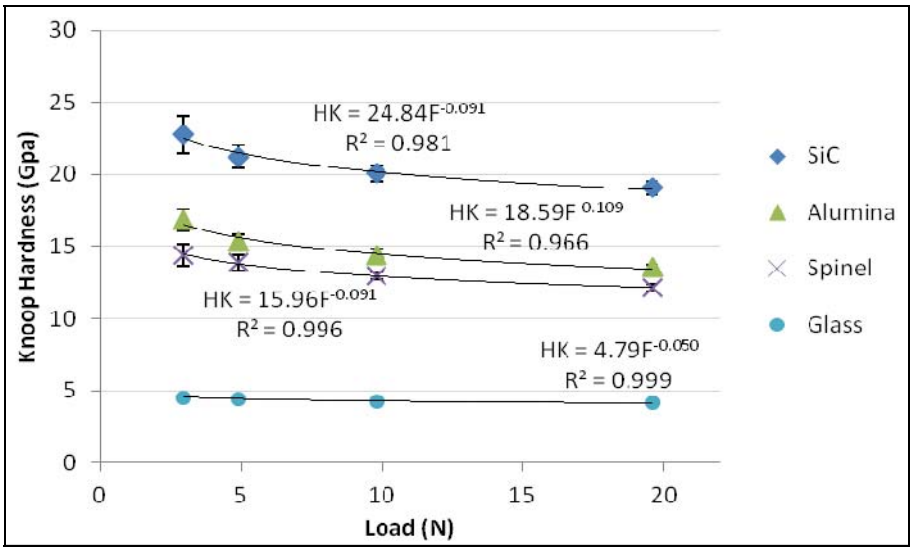

Figure 5. Typical hardness-load curves for four materials.

New data (based on hardness tests on SiC-N, SiC-HPN, and SiC-X1) obtained recently has allowed a refinement of the predictive equation. Better overall agreement is achieved between the TV values that are predicted by the approach and those that are measured in experiments (*34*). The refined equation has new constants, as shown in equation 4:

$$TV = 33.59\ [\text{Hardness (1 N)} + \text{Abs (1/c)}] + 261.42\ . \qquad (4)$$

This new equation also appears to predict the behavior of the SiC materials well, while it is less accurate with AlON. This may indicate that the current predictive equation is applicable to most fully dense, hard SiC materials. The differences between predicted and measured TVs for AlON may be a result of the coarse-grained (200+ μm) microstructure of the material. In AlON, it is likely that entire indentations fall within a single grain at the lower loads compared to fine-grained SiC materials, where many grains are indented.

4.2 Bulk Plasticity Calculations/TV Predictions

Table 1 shows a summary of the results obtained in (*34*) for those materials for which the TV has been measured experimentally. Various SiC materials are included along with ALON. As previously stated, the hardness tests were performed by four operators* using three different hardness testing units. The operators are represented by the numbers 1 through 5 in the "Operator" column of the table, while the hardness testers are represented by the letters A through C in the final column. "Abs. (1/c)" represents the absolute value of the reciprocal of the c exponent from the power-law equation (equation 1). All of the R^2 values are above 0.90, with most higher than 0.95. This indicates that the power law equation effectively represents the hardness-load data that was used to create the table.

*In addition to the data generated by four operators in the current study, data from previous studies by McCauley and Wilantewicz (*28*) are included for SiC-N, SiC-SC-1RN, and SiC-HPN.

Table 1. Summary of plasticity + hardness calculations and TV comparisons (predicted vs. measured).

Material	Operator	Abs. (1/c)	R^2	HK(1N)	HK(1N) + Abs. (1/c)	Predicted TV (m/s)	Measured TV (m/s)	% Diff	Hardness Tester
SiC-N	1	10.75	0.997	25.54	36.29	1480 ± 54	1507 ± 5	1.79	A
	2	12.35	0.982	25.09	37.43	1519 ± 81		0.80	A
	3	11.11	0.993	26.76	37.87	1533 ± 40		1.73	B
	4	6.90	0.964	30.69	37.58	1524 ± 30		1.13	B
	5	15.15	0.920	22.40	37.55	1523		1.06	C
SiC-SC-1RN	2	9.90	0.988	26.52	36.42	1485 ± 21	1526 ± 25	2.69	A
	3	9.09	0.934	27.26	36.35	1482 ± 19		2.88	B
	4	10.64	0.931	25.70	36.34	1482 ± 54		2.88	A
	5	15.15	0.961	22.90	38.05	1540		0.92	C
SiC-HPN	2	12.66	0.950	25.25	37.91	1535 ± 40	1625 ± 12	5.54	A
	3	7.87	0.996	29.55	37.42	1518 ± 11		6.58	B
	4	12.05	0.935	26.71	38.76	1563 ± 46		3.82	B
	5	19.23	0.994	22.50	41.73	1663		2.34	C
SiC-X1	2	10.42	0.913	25.89	36.30	1481 ± 51	1517 ± 17	2.37	A
	3	9.43	0.965	28.70	38.13	1542 ± 21		1.65	B
	4	14.71	0.943	23.58	38.29	1547 ± 97		1.98	B
AlON	1	9.62	0.979	18.78	28.39	1215 ± 40	1207 ± 35	0.66	B
	2	15.63	0.916	17.09	32.71	1360 ± 86		12.68	A
	3	11.36	0.994	18.93	30.29	1279 ± 56		5.97	B
	3	15.15	0.995	17.76	32.91	1367 ± 126		13.26	B
	4	7.63	0.967	20.12	27.75	1194 ± 19		1.08	A

The uncertainty values shown in table 1 for the predicted TVs were determined using the method developed by Portune and Hilton (*36*). This method applies Bayesian hypothesis testing to probability distributions for hardness values at each applied load to define a joint likelihood function for Meyer's Law parameters k and c. The McCauley-Wilantewicz method is applied to this function to create likelihood functions for the plasticity parameter and the TV. In previous studies, this distribution was typically asymmetric and unimodal (*37*). The uncertainty values in the "Predicted TV" column in table 1 represent the region surrounding the peak maximum that corresponds to 67% of the total probability for the TV likelihood function. That percentage was chosen to correspond most closely to a single standard deviation in a Gaussian distribution. In most cases, the uncertainty was within 5% of the expected value for both the plasticity parameter and the estimated TV.

The "% Diff" column in table 1 shows the percentage difference between the TV values predicted by equation 4 and those measured in reverse-impact experiments. Excellent agreement between the two quantities is generally observed, especially for the SiC materials, for which the difference between the predicted and measured TVs is less than 5% in most instances. As previously suggested, the larger differences observed between the predicted and the measured TVs for AlON may be a result of the ceramic's coarse microstructure.

Table 1 also illustrates the robustness of the technique. While the predicted and measured TVs are in excellent agreement for all operators and hardness testers, the values of the plasticity parameter for a given ceramic vary from operator to operator. For AlON, even the same operator can obtain different values. These differences in plasticity, however, are offset by the extrapolated HK (1N) values. This demonstrates that differences in operator experience with hardness testing, and/or between hardness testing units, do not significantly affect the technique's potential for accurate TV predictions.

TVs for Al_2O_3 ceramics are predicted in table 2 and plotted in figure 6. Figure 6a represents all of the Al_2O_3 materials in table 2, grouped according to manufacturer. The predicted TVs for these ceramics range from nearly 1000 m/s up to approximately 1400 m/s. Figure 6b displays predicted TVs for the different Al_2O_3 materials manufactured by CoorsTek. This figure illustrates the current technique's potential for distinguishing between variations of a particular type of ceramic and further demonstrates the robustness of the technique. For those materials tested by at least two operators (shown by at least two bars), similar TV predictions were obtained. The fact that the predictions do not show a strong dependence on the operator adds credibility to conclusions regarding trends in observed behaviors. For instance, it may be anticipated that the SA-999-1 material may perform relatively well as an armor ceramic, while less may be expected from the AD-85-S1 or AD-94-A2 materials. In addition, it should be noted that, in most cases, similar uncertainties in predicted TV (represented by error bars in the figure) are observed for each of the Al_2O_3 materials. These uncertainties likely reflect the microstructural heterogeneity that exists in these ceramics. Accordingly, one may expect the microstructure of sample AD-96-IWB, for example, to be less variable than sample AD-90-S2. It should be mentioned that some of the R^2 values observed in the current study are relatively low, reflecting poor agreement between the HK-load data and the power law fit. More confidence should be placed in those TV predictions that are associated with R^2 values ≥ 0.95.

Table 2. Details of plasticity/TV calculations for various alumina materials.

Manufacturer	ID	Operator	Abs.(1/c)	R^2	HK(1N)	HK(1N) + Abs.(1/c)	Predicted TV (m/s)	Hardness Tester
BAE	Ebon A	3	13.89	0.994	19.73	33.62	1391 ± 64	B
Bitossi	3815585-7-4 NH	3	10.00	0.997	20.46	30.46	1285 ± 35	B
	38-PT13585-12 NH	3	8.26	0.986	22.05	30.31	1280 ± 16	B
	38-PT-15-10-1 NH	4	9.62	0.997	20.27	29.89	1265 ± 30	B
	38-PT7 HIP 30 NH	3	12.82	0.994	20.46	33.28	1380 ± 56	B
	38-PT7 HIP'ed 1300C	3	10.53	0.992	21.66	32.19	1343 ± 38	B
	38-PT7-25 HIP'ed 1585C	3	10.00	0.983	22.65	32.65	1358 ± 24	B
	41-PT711-6-4 NH	3	10.31	0.953	20.01	30.32	1280 ± 40	B
	41-PT711-6-8 HIP'ed 1585C	3	9.90	0.991	22.00	31.9	1333 ± 40	B
	41-ZH	4	9.17	0.948	19.21	28.38	1215 ± 43	B
	FS 6215-1 NH	3	12.82	0.995	17.71	30.53	1287 ± 83	B
	FS 6215-7 HIP'ed 1300C	3	9.09	0.978	19.78	28.87	1231 ± 32	B
	FS STD-29-F1 NH	3	11.49	0.978	18.63	30.12	1273 ± 62	B
	FS15-10-F1 NH	3	9.62	0.987	18.41	28.03	1203 ± 67	B
Ceradyne	2 µm	3	15.38	0.977	18.74	34.12	1408 ± 113	B
		1	13.70	0.820	19.01	32.71	1360 ± 89	A
	15 µm	3	17.54	0.956	17.39	34.93	1435 ± 121	B
		1	13.16	0.664	19.32	32.48	1353 ± 86	B
	25 µm	3	11.24	0.985	17.27	28.51	1219 ± 59	B
		1	6.13	0.994	27.53	33.66	1392 ± 27	B
CoorsTek	AD-85-S	3	6.62	0.955	14.95	21.57	986 ± 19	B
	AD-85-SI	1	5.03	0.880	16.79	21.82	994 ± 35	B
	AD-85-SI	3	6.37	0.987	15.40	21.77	993 ± 30	B
	AD-90-S2	1	11.9	0.792	12.91	24.81	1095 ± 78	B
	AD-90-S2	3	13.16	0.985	14.22	27.38	1181 ± 89	B
	AD-94-A2	1	6.90	0.622	16.84	23.74	1059 ± 32	B
	AD-94-A2	3	8.33	0.900	16.36	24.69	1091 ± 35	B
	AD-96-IWB	1	7.63	0.899	18.18	25.81	1128 ± 27	B
	AD-96-IWB	3	8.33	0.991	16.77	25.1	1105 ± 27	B
	AD-995-I2	4	10.99	0.892	18.30	29.29	1245 ± 54	B
	AD-995-I2	1	8.7	0.905	20.55	29.25	1244 ± 35	B
	AD-995-I2	3	9.52	0.992	19.05	28.57	1221 ± 21	B
	AD-999	3	10.99	0.978	21.28	32.27	1345 ± 48	B
	FG-98-S	3	9.71	0.989	16.76	26.47	1151 ± 35	B
	FG-995-S2	3	9.17	0.986	16.73	25.9	1131 ± 38	B
	FG-995-S2	1	5.81	0.852	20.29	26.1	1138 ± 40	B
	SA-999-1	3	10.53	0.994	20.81	31.34	1314 ± 30	B
	SA-999-1	4	9.52	0.947	21.06	30.58	1289 ± 32	B
	SA-999-1	1	10.42	0.908	21.50	31.92	1334 ± 40	B

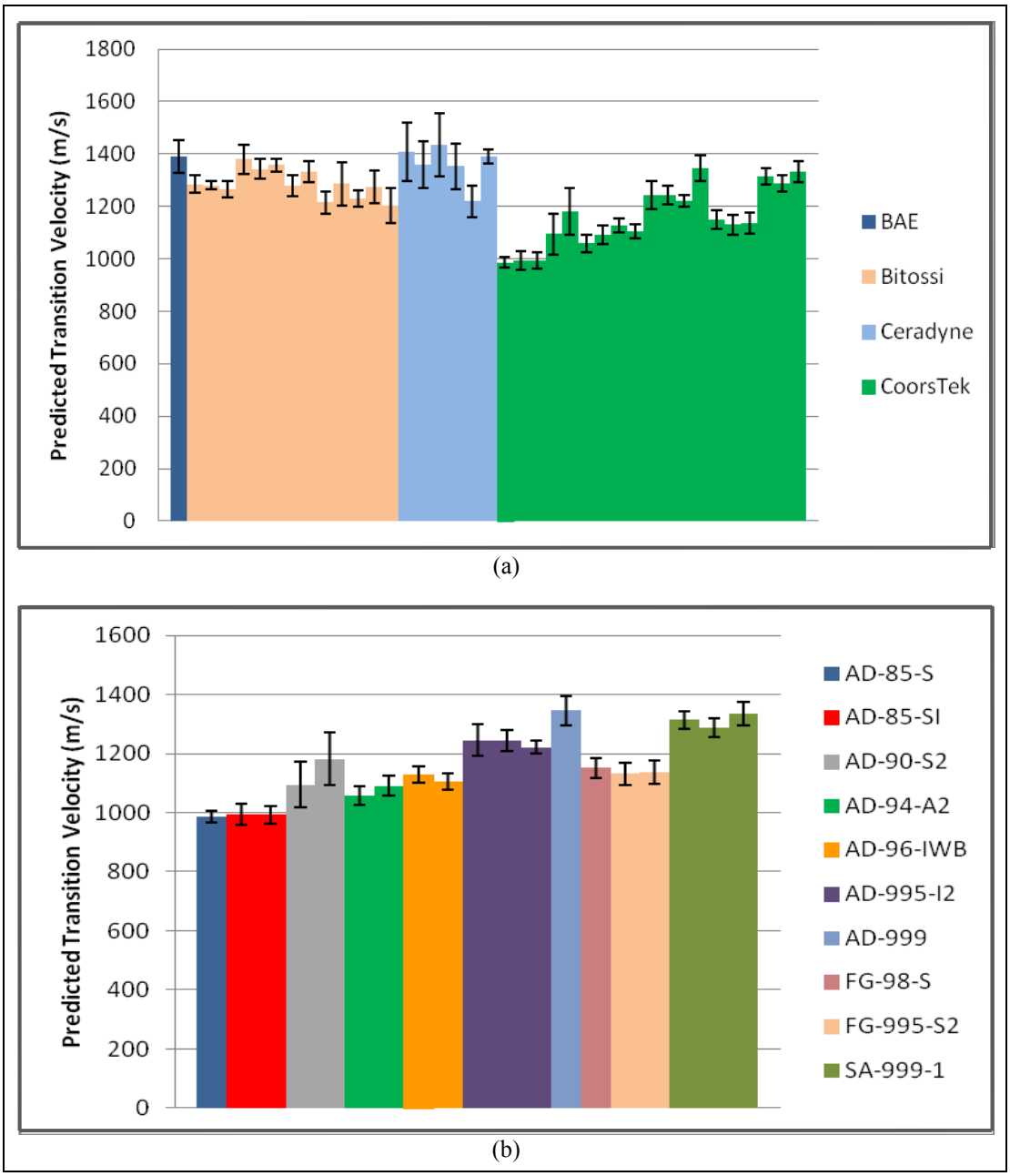

Figure 6. Predicted TVs for various Al_2O_3 materials, grouped by manufacturer (a), and predicted TVs for various CoorsTek Al_2O_3 materials (b).

Predicted TV values for additional materials are shown in table 3 and plotted in figure 7. Although multiple operators, hardness testing units, and material variations are represented within each material class, some general trends are evident. Cubic BN is predicted to have the best impact resistance, with TVs of 2574 and 1892 m/s, while the lowest TV values (as low as 1026 m/s) are observed in the glass materials (although the predicted TVs for glasses depend on the particular type of glass). Significant disparity exists between the two operators in predicted velocities for the Cubic BN materials. Therefore, further testing should be carried out on this

material in order to gain confidence in TV predictions. Si_3N_4 and Spinel are predicted to perform slightly better than the inferior, Starfire glasses. Velocities near 1400 m/s are predicted for the B_4C/SiC composites—similar to the velocities predicted for the Al_2O_3 ceramics produced by BAE and Ceradyne, and the CeraLumina material produced by Ceranova. B_4C (and boron-rich boron carbide [*38*]), SiC, and WC are all predicted to perform relatively well. In general, the calculated TVs for these ceramics are above 1500 m/s, with WC predicted to surpass 1850 m/s in some cases.

Table 3. Details of plasticity/TV calculations for various ceramic and glass materials.

Material	Manufacturer	ID	Operator	Abs.(1/c)	R^2	HK(1N)	HK(1N) + Abs.(1/c)	Predicted TV (m/s)	Hardness Tester
AlN	BAE		3	18.52	0.810	12.18	30.70	1293	B
	Dow Chemical		3	30.30	0.878	10.50	40.80	1632	B
B_4C	Ceradyne	546 02-3706	3	9.01	0.978	27.59	36.60	1491 ± 30	B
	Ceradyne		1	6.62	0.975	31.66	38.28	1547 ± 32	B
	Cercom	02-2177	3	10.53	0.999	28.35	38.88	1567 ± 40	B
	Cercom		1	7.94	0.968	31.03	38.97	1570 ± 46	B
B_4C/SiC Composite		BSC-400	4	4.90	0.973	28.13	33.03	1371 ± 72	B
		BSC-400	3	8.62	0.928	25.20	33.82	1397 ± 19	B
		BSC-800	4	11.63	0.926	23.11	34.74	1428 ± 51	B
		BSC-800	3	5.75	0.967	29.07	34.82	1431 ± 43	B
		RBBC-751	4	10.20	0.615	21.34	31.54	1321 ± 59	B
		RBBC-751	3	5.21	0.930	26.65	31.86	1332 ± 70	B
Boron Rich B_4C		10% B 2-385-4	3	9.62	0.969	28.52	38.14	1543 ± 27	B
		33% B 2-385-3	3	8.06	0.962	29.92	37.98	1537 ± 16	B
		43% B 2-385	3	9.01	0.998	28.38	37.39	1517 ± 27	B
		43% B 2-428-1	3	11.90	0.990	26.63	38.53	1556 ± 64	B
		43% B 2-428-3	3	9.80	0.962	27.93	37.73	1529 ± 32	B
		55% B 2-385	3	8.85	0.987	29.86	38.71	1562 ± 24	B
Cubic BN			1	4.42	0.982	64.44	68.86	2574	A
			3	7.09	0.905	41.45	48.54	1892 ± 40	B
Glass		Borofloat	2	17.86	0.857	4.89	22.75	1026	A
		Borofloat	4	20.00	0.999	4.79	24.79	1094 ± 105	B
		Starfire SLS	2	29.41	0.975	4.91	34.32	1414 ± 129	A
		Starfire SLS	4	28.57	0.938	4.81	33.38	1382	B
Si_3N_4	Ceradyne	147-31N	4	9.17	0.966	18.59	27.76	1194 ± 32	B
		NC-132	4	8.93	0.952	19.87	28.80	1229 ± 30	B
SiC	CoorsTek	SC-30	3	13.33	0.992	25.91	39.24	1579 ± 72	B
	Saint Gobain	Hexoloy SA - SWB	4	8.33	0.944	26.97	35.30	1447 ± 21	B
	Verco	Sintered/HIP	3	15.63	0.992	26.40	42.03	1673 ± 91	B
		Ekasic-F	3	12.50	0.958	27.39	39.89	1601 ± 54	B
		Ekasic-F+	3	9.01	0.981	29.66	38.67	1560 ± 13	B
		Ekasic-T	3	10.00	0.959	26.60	36.60	1491 ± 21	B
		High Pressure HIP	3	18.87	0.991	16.52	35.39	1450 ± 83	B
		Standard HIP	3	19.61	0.981	16.75	36.36	1483 ± 94	B
SiC-N Cube	BAE	2-1-4	4	5.78	0.950	27.58	33.36	1382 ± 27	B
		6-2	4	10.20	0.949	25.46	35.66	1459 ± 35	B
		6-5	4	13.70	0.996	23.51	37.21	1511 ± 80	B
		6-8	4	10.99	0.981	24.84	35.83	1465 ± 62	B
		6-10	4	9.26	0.945	25.93	35.19	1443 ± 30	B
		6-12	4	12.82	0.904	24.12	36.94	1502 ± 64	B
		6-13	4	8.85	0.961	27.12	35.97	1470 ± 27	B
CeraLumina	Ceranova	800 nm	3	9.62	0.959	23.90	33.52	1387 ± 24	B
		450 nm	3	8.13	0.976	25.10	33.23	1378 ± 16	B
Spinel	Krell	0.5 micron	4	10.87	0.978	15.98	26.85	1163 ± 51	B
	Krell	0.5 micron	3	13.33	0.897	15.83	29.16	1241 ± 70	B
	Krell	1.5 micron	2	12.66	0.955	15.30	27.96	1201 ± 99	A
	Krell	1.5 micron	4	11.90	0.961	15.35	27.25	1178 ± 70	B
	TA&T	1.0 - LiF	3	12.66	0.965	16.31	28.97	1234 ± 80	B
	TA&T	1.25 - LiF	3	14.08	0.958	15.64	29.72	1260 ± 102	B
		030T	4	10.99	0.977	15.45	26.44	1150 ± 64	B
		030MT	4	11.90	0.987	15.43	27.33	1179 ± 72	B
		030MB	4	9.52	0.987	16.14	25.66	1123 ± 46	B
		102B	3	8.55	0.955	17.27	25.82	1129 ± 24	B
		104M	3	14.49	0.988	15.92	30.41	1283 ± 80	B
		152B	3	12.05	0.986	15.29	27.34	1180 ± 59	B
		161MB	3	12.35	0.982	15.91	28.26	1211 ± 51	B
		94M	3	8.20	0.994	17.81	26.01	1135 ± 27	B
		95M	3	10.53	0.919	16.46	26.99	1168 ± 54	B
TiB_2			4	6.17	0.999	26.09	32.26	1345 ± 56	B
		SWB	4	5.99	0.997	27.81	33.80	1397 ± 38	B
WC	Cercom		4	12.35	0.920	25.38	37.73	1529 ± 48	B
	Kennametal	RocTec 500	4	12.05	0.936	29.15	41.2	1645 ± 51	B
	Sandvik		4	13.16	0.977	22.22	35.38	1450 ± 67	B

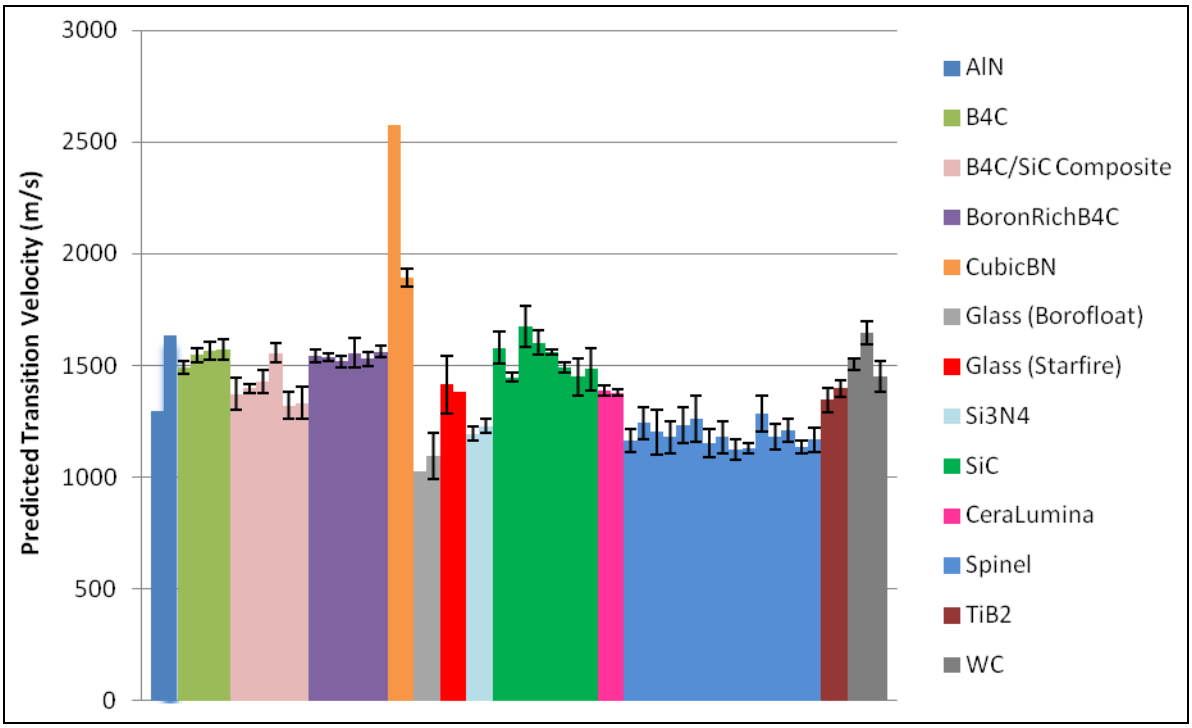

Figure 7. Predicted TVs for various ceramic and glass materials.

The uncertainty estimates in the predicted TVs are largest in the glass materials. While standard deviations in the ceramic materials were less than 80 m/s in the large majority of materials, the standard deviations in the predicted TVs for the glasses were above 100 m/s in two of the four data sets. Furthermore, in the remaining two glass data sets, uncertainty values could not be determined.* The applicability of this approach to glass materials may therefore be questionable.

Further reverse impact testing is required to validate the predicted TVs for the materials in tables 2 and 3. As previously mentioned, the current approach seems to work well for dense, hard, SiC materials. However, caution must be exercised when examining predictions for other materials. As previously discussed, the applicability of the method to AlON and glass may be questionable. It is possible, however, that slight modifications to the approach may extend its applicability to other classes of ceramics. For example, the constants of the predictive equation (equation 4) may change according to the specific class of ceramic under investigation. One pair of constants may work well for SiC materials, while another pair may provide accurate predictions for Al_2O_3 materials. Additionally, it may be useful to gain an understanding of the influence that variables such as grain size, grain boundary phases, fracture toughness, and tensile strength may have on the efficacy of the approach. Consideration of these variables may allow for further refinement of the method and extend its applicability to a wider range of ceramic materials.

*Uncertainties in the predicted TVs could not be determined for a few of the materials contained in table 3. This was due to an atypical degree of asymmetry in the associated TV likelihood functions.

5. Conclusions

The results of the current study further validate the approach described in McCauley and Wilantewicz (*28*) and support the importance of hardness and plasticity in the impact performance of ceramic materials. More specifically, the potential of these two factors for predicting transition velocities of ceramics has been demonstrated. Generally speaking, the TV values predicted by the approach are remarkably accurate. In most cases, the TVs measured in Lundberg's experiments can be predicted to within 5% for the SiC materials. Less accurate predictions were obtained for AlON—likely a result of the large grains (200+ μm) in this material. Future investigations will focus on the effects of variables such as grain size, grain boundary phases, and fracture toughness on the accuracy of predictions. This may allow further refinement of the approach and thereby extend its applicability to a wider range of materials. The current study demonstrates the robustness of the technique through its application to a variety of armor ceramics (Al_2O_3, SiC, Spinel, etc.). Although results of hardness tests can depend on many factors (operator experience, testing unit, etc.), similar TV predictions (and similar uncertainties) were obtained by multiple operators using multiple hardness testing units. This is a desirable characteristic, as it shows that this method can be confidently utilized without significant regard to the experience of the operator or the capabilities of the hardness tester.

The plasticity index/predictive technique described here is a simple method that could be extremely useful as a screening tool for prospective ceramic armor materials by allowing researchers to quickly identify and rank them. This could significantly benefit experimentalists conducting system-level impact tests by allowing them to test only the most promising ceramics, thereby avoiding the time and expense associated with investigating materials that show less potential. Further refinement and validation of the predictive technique discussed here could lead to its use as an aid in guiding the development of new, superior armor ceramics.

6. References

1. Viechnicki, D.; Bluementhal, W.; Slavin, M.; Tracy, C.; Skeele, H. Armor Ceramics - 1987. Presented at the Third TACOM Armor Coordinating Conference, Monterey, CA, 1987.

2. Flinders, M.; Ray, D.; Anderson, A.; Cutler, R. High-Toughness Silicon Carbide as Armor, *J. of the American Ceramic Society* **2005**, *88*, 2217–2226.

3. Krell, A.; Strassburger, E. High-Purity Submicron alpha-Al_2O_3 Armor Ceramics: Design, Manufacture, and Ballistic Performance. *Ceramic Transactions* **2001**, *134*, 463–471.

4. Roberson, C.; Hazell, P. J. Resistance of Different Ceramic Materials to Penetration by a Tungsten Carbide Cored Projectile. *Ceramic Transactions* **2006**, *151*, 153–163.

5. Sternberg, J. Material Properties Determining the Resistance of Ceramics to High Velocity Penetration. *J. Appl. Phys.* **1989**, *65* (9), 3417–3424.

6. LaSalvia, J. C.; Horwath, E. J.; Rapacki, E. J.; Shih, C. J.; Meyers, M. A. Microstructural and Micromechanical Aspects of Ceramic/Long-Rod Projectile Interactions: Dwell/Penetration Transitions. Presented at Explomet 2000, Albuquerque, NM, 2000.

7. LaSalvia, J. C.; Campbell, J.; Swab, J. J.; McCauley, J. W. Beyond Hardness: Ceramics and Ceramic-Based Composites for Protection. *JOM* **2010**, *62* (1), 16–23.

8. Lundberg, P.; Renstrom, R.; Lundberg, B. Impact of Metallic Projectiles on Ceramic Targets: Transition Between Interface Defeat and Penetration. *Intrntl. J. of Impact Engrg.* **2000**, *24*, 259–275.

9. Wilkins, M. L.; Cline, C. F.; Honodel, C. A. *Light Armor*; UCRL-71817; Lawrence Radiation Laboratory, University of California: Livermore, CA, 1969.

10. Magnusson, P.; Shen, Z. Ceramic Based Nanomaterials for Ballistic Protection. In *Nanomaterials Technology for Military Vehicle Structural Applications*; Neuilly-sur-Seine, France, 2005; pp 12-1–12-8.

11. Hockey, B. J. Plastic Deformation of Aluminum Oxide by Indentation and Abrasion. *J. Am. Ceram. Soc*. **1971**, *54* (5), 223–231.

12. Yang, K. H.; Ho, N.-J.;. Lu, H.-Y. Deformation Microstructure in (001) Single Crystal Strontium Titanate by Vickers Indentation. *J. Am. Ceram. Soc*. **2009**, *92* (10), 2345–2353.

13. Zhang, H.; Fang, Z. Z.; Belnap, J. D. Quasi-Plastic Deformation of WC-Co Composites Loaded with a Spherical Indenter. *Metallurgical and Materials Transactions A* **2007**, *38A* 552–561.

14. Bull, S. J. Using Work of Indentation to Predict Erosion Behavior in Bulk Materials and Coatings. *J. of Physics D: Applied Physics* **2006**, *39*, 1626–1634.

15. Guo, J. J.; Wang, K.; Fujita, T.; McCauley, J. W.; Singh, J. P.; Chen, M. W. Nanoindentation Characterization of Deformation and Failure of Aluminum Oxynitride. *Acta Materialia* **2011**, *59*, 1671–1679.

16. Chan, H. M.; Lawn, B. R. Indentation Deformation and Fracture of Sapphire. *J. Am. Ceram. Soc*. **1988**, *71* (1), 29–35.

17. LaSalvia, J. C.; McCauley, J. W. Inelastic Deformation Mechanisms and Damage in Structural Ceramics Subjected to High-Velocity Impact. *Int. J. Appl. Ceram. Technol*. **2010**, *7* (5), 595–605.

18. Milman, Y. Plasticity Characteristic Obtained by Indentation. *J. Phys. D: Appl. Phys*. **2008**, *41*.

19. Lawn, B. R.; Howes, V. R. Elastic Recovery at Hardness Indentations. *J. of Materials Science* **1981**, *16*, 2745–2752.

20. McColm, I. J. *Ceramic Hardness*; Plenum Press: New York, NY, 1990.

21. Chen, J.; Bull, S. J. A Critical Examination of the Relationship between Plastic Deformation Zone Size and Young's Modulus to Hardness Ratio in Indentation Testing. *J. Mater. Res*. **2006**, *21* (10), 2617–2627.

22. Sakai, M. Simultaneous Estimate of Elastic/Plastic Parameters in Depth-Sensing Indentation Tests. *Scripta Materialia* **2004**, *51*, 391–395.

23. Wilantewicz, T. E.; McCauley, J. W. Analysis of Hardness Indentation Size Effect (ISE) Curves in Ceramics: A New Approach to Determine Plasticity. *Advances in Ceramic Armor IV* **2009**, *29* (6), 219–227.

24. Quinn, J. B.; Quinn, G. D. Indentation Brittleness of Ceramics: A Fresh Approach. *J. Mat. Sci*. **1997**, *32*, 4331–4443.

25. Sargent, P. M. Use of the Indentation Size Effect on Microhardness for Materials Characterization. In *Microindentation Techniques in Materials Science and Engineering*, Blau, P. J., Lawn, B. R., Eds.; American Society for Testing and Materials: Philadelphia, PA, 1986; pp 160–174.

26. Li, H.; Bradt, R. C. The Microhardness Indentation Load/Size Effect in Rutile and Cassiterite Single Crystals. *J. Mat. Sci*. **1993**, *28*, 917–926.

27. Swab, J. J. Recommendations for Determining the Hardness of Armor Ceramics. *Int. J. Appl. Ceram. Technol*. **2004**, *1* (3), 219–225.

28. McCauley, J.; Wilantewicz, T. *Using Plasticity Values Determined From Systematic Hardness Indentation Measurements for Predicting Impact Behavior in Structural Ceramics: A New Simple Screening Technique*; ARL-RP-268; U.S. Army Research Laboratory: Aberdeen Proving Ground, MD, September 2009.

29. Meyer, E. Investigations of Hardness Testing and Hardness. *Phys. Z.* **1908**. *9* (66).

30. Ren, X. J.; Hooper, R. M.; Griffiths, C.; Henshall, J. L. Indentation Size Effect in Ceramics: Correlation with H/E. *J. of Materials Science Letters* **2003**, *22*, 1105–1106.

31. Hauver, G. E.; Netherwood, P. H.; Benck, R. F.; Kecskes, L. J. Enhanced Ballistic Performance of Ceramic Targets. In *Army Science Conference*, U.S. Army, 1994.

32. Lundberg, P.; Anderson, O. *Experimental Study of the Dwell-Penetration Transition in SiC-X1 and AlON*; FOI-2009-1179; Final Report, Swedish Defence Research Agency, Kista, Sweden, February 2010.

33. Lundberg, P.; Lundberg, B. Transition Between Interface Defeat and Penetration for Tungsten Projectiles and Four Silicon Carbide Materials. *Int. J. of Impact Engrg*. **2005**, *31*, 781–792.

34. Hilton, C.; McCauley, J.; Swab, J.; Shanholtz, E. Using Hardness Tests to Quantify Bulk Plasticity and Predict Transition Velocities in SiC Materials. *Int. J. Appl. Ceram. Technol. (accepted for publication)*, 2012.

35. ASTM C 1326-03. Standard Test Method for Knoop Indentation of Advanced Ceramics. *ASTM Book ASTM Stand.* **2003**.

36. Portune, A.; Hilton, C. Quantifying Uncertainty in Load-Hardness Relationships. *J. of Materials Science* **2012,** *47* (12), 4851–4859.

37. Portune, A.; Hilton, C. Determination of Uncertainty in Transition Velocity Estimates for Ceramic Materials. *Int. J. Appl. Ceram. Technol. (accepted for publication)*, 2011.

38. Chheda, M.; Shih, J.; Gump, C.; Buechler, K.; Weimer, A. *Synthesis and Processing of Boron-Rich Boron Carbide*; Ceradyne Inc., Costa Mesa, CA, 2001.

NO. OF COPIES	ORGANIZATION
1 (PDF only)	DEFENSE TECHNICAL INFORMATION CTR DTIC OCA 8725 JOHN J KINGMAN RD STE 0944 FORT BELVOIR VA 22060-6218
1	DIRECTOR US ARMY RESEARCH LAB IMNE ALC HRR 2800 POWDER MILL RD ADELPHI MD 20783-1197
1	DIRECTOR US ARMY RESEARCH LAB RDRL CIO LL 2800 POWDER MILL RD ADELPHI MD 20783-1197

NO. OF COPIES	ORGANIZATION
1	OSD OUSD (A&T) ODDR&E (W) L SLOTER 1777 N KENT ST STE 9030 ARLINGTON VA 22209
1	COMMANDER SMCWV QAE Q B VANINA BLDG 44 WATERVLIET ARSENAL WATERVLIET NY 12189-4050
1	PM HBCT SFAE GCS HBCT S J ROWE 6501 11 MILE RD MS 506 WARREN MI 48397-5000
2 (CD only)	PM STRYKER SFAE GCS BCT M RYZYI 6501 EAST 11 MILE RD MS 325 WARREN MI 48397-5000
1	PM HEAVY BRIGADE COMBAT TEAM SFAE CGSS W AB QT J MORAN 6501 EAST ELEVEN MILE RD WARREN MI 48397-5000
1 (CD only)	SARDA OFC OF DEPUTY ASST SEC ARMY R&D J PARMENTOLA PENTAGON WASHINGTON DC 20301-0103
1	US ARMY ATCOM AVIATION APPLD TECHL DIR J SCHUCK FT EUSTIS VA 23604
1	US ARMY MIS LAB AMSMI RD AS MM M MULLINS REDSTONE ARSENAL AL 35809
1	US ARMY RDECOM AMSRD TAR R L PROKURAT-FRANKS 6501 E ELEVEN MILE RD MS 263 WARREN MI 48397-5000
1	US ARMY RDECOM AMSTAR TR R K BISHNOI 6501 E ELEVEN MILE RD MS 263 WARREN MI 48397-5000
1	DIRECTOR US ARMY RSRCH LAB RDRL ROE A M RAJENDRAN PO BOX 12211 RESEARCH TRIANGLE PARK NC 27709-2211
1	US ARMY TACOM ARDEC RDAR MEE W E BAKER BLDG 3022 PICATINNY ARSENAL NJ 07806-5000
1	USA SBCCOM PM SOLDIER SPT AMSSB PM RSS A J CONNORS KANSAS ST NATICK MA 01760-5057
1	NAV SURFC WARFARE CTR CARDEROCK DIV CODE 28 R PETERSON 9500 MACARTHUR BLVD WEST BETHESDA MD 20817-5700
3	AIR FORCE ARMAMENT LAB AFATL DLJW D BELK W COOK J FOSTER EGLIN AFB FL 32542
1	LAWRENCE LIVERMORE NATL LAB L 372 R LANDINGHAM PO BOX 808 LIVERMORE CA 94550
1	LAWRENCE LIVERMORE NATL LAB L 282 J REAUGH PO BOX 808 LIVERMORE CA 94551-5554

NO. OF COPIES ORGANIZATION

1 SANDIA NATIONAL LAB
MS 0378
M KIPP
PO BOX 5800
ALBUQUERQUE NM 87185

1 SANDIA NATL LAB
MS 0836 9116
D CRAWFORD
PO BOX 5800
ALBUQUERQUE NM 87185-5800

2 SANDIA NATL LABS
J ASAY MS 1181
L CHHABILDAS MS 1181
PO BOX 5800
ALBUQUERQUE NM 87185-5800

1 NATL INST OF STAND & TECH
CRMCS DIV
G QUINN
STOP 852
GAITHERSBURG MD 20899

2 CALTECH
G RAVICHANDRAN
T AHRENS MS 252 21
1201 E CALIFORNIA BLVD
PASADENA CA 91125

1 JHU MECH ENG
K T RAMESH
223 LATROBE HALL
3400 N CHARLES ST
BALTIMORE MD 21218

1 RUTGERS THE STATE UNIV
OF NEW JERSEY
DEPT OF CRMCS & MATLS ENGRNG
R HABER
607 TAYLOR RD
PICATINNY NJ 08854

1 SOUTHWEST RSRCH INST
J P RIEGEL
6220 CULEBRA RD
PO DRAWER 28510
SAN ANTONIO TX 78228-0510

1 UNIV OF DELAWARE CTR FOR
COMPOSITE MATERIALS
J GILLESPIE
201 SPENCER LAB
NEWARK DE 19716

NO. OF COPIES ORGANIZATION

1 UNIV OF TEXAS INST FOR ADVNCD
TECH
S BLESS
3925 W BRAKER LN
AUSTIN TX 78759-5316

1 UNIVERSITY OF DAYTON RSRCH
INST
MS SPC 1911
N S BRAR
300 COLLEGE PARK
DAYTON OH 45469

2 WASHINGTON ST UNIV
INST OF SHOCK PHYSICS
J ASAY
Y M GUPTA
PULLMAN WA 99164-2814

1 APPLIED RSRCH ASSOCIATES
D GRADY
4300 SAN MATEO BLVD NE STE A220
ALBUQUERQUE NM 87110

1 BOB SKAGGS CONSULTANT
S R SKAGGS
7 CAMINO DE LOS GARDUNOS
SANTA FE NM 87506

3 CERADYNE
B MIKIJELJ
Z NAWAZ
M NORMANDIA
3169 REDHILL AVE
COSTA MESA CA 92626

3 CERANOVA
N CORBIN
M PARISH
M PASCUCCI
85 HAYES MEMORIAL DR
MARLBOUROUGH MA 01752

2 COORSTEK VISTA OPERATIONS
D ASHKIN
R PALICKA
2065 THIBOBO RD
VISTA CA 92081

1 GENERAL DYNAMICS LAND SYS
MZ436 20 29
D DEBUSSCHER
38500 MOUND RD
STERLING HEIGHTS MI 48313

NO. OF COPIES	ORGANIZATION
1	GLDS MZ436 01 24 W HERMAN 38500 MOUND RD STERLING HEIGHTS MI 48310-3200
3	GLDS MZ436 21 24 W BURKE J ERIDON S PENTESCU 38500 MOUND RD STERLING HEIGHTS MI 48310-3200
1	GLDS MZ436 30 44 G CAMPBELL 38500 MOUND RD STERLING HEIGHTS MI 48310-3200
1	INTERNATIONAL RSRCH ASSOC INC D ORPHAL 4450 BLACK AVE STE E PLEASANTON CA 94566
1	JET PROPULSION LAB IMPACT PHYSICS GROUP M ADAMS 4800 OAK GROVE DR PASADENA CA 91109-8099
3	OGARA HESS & EISENHARDT G ALLEN D MALONE T RUSSELL 9113 LE SAINT DR FAIRFIELD OH 45014
2	SIMULA INC V HORVATICH V KELSEY 10016 51ST ST PHOENIX AZ 85044
1	SOUTHWEST RSCH INST K DANNEMANN 6220 CULEBRA RD DRAWER 28510 SAN ANTONIO TX 78284
4	SOUTHWEST RSRCH INST ENGRG AND MAT SCI DIV C E ANDERSON T HOLMQUIST G JOHNSON J WALKER 6220 CULEBRA RD PO DRAWER 28510 SAN ANTONIO TX 78228-0610
3	SRI INTERNATIONAL D CURRAN R KLOOP D A SHOCKEY 333 RAVENSWOOD AVE MENLO PARK CA 94025-3493
5	TECHLGY ASSESSMENT & TRANSFER INC L FEHRENBACKER J KUTSH A LAROCHE L RENOMERON I VESNOVSKY 215 NAJOLES RD MILLERSVILLE MD 21108
2	UNITED DEFENSE LP E BRADY R JENKINS PO BOX 15512 YORK PA 17405-1512
1	UNITED DEFNS LIMITED PARTNERS GROUND SYS DIV K STRITTMATTER PO BOX 15512 YORK PA 17405-1512
2	US ARMY RSRCH OFC RDRL ROE M B LAMATINA D STEPP PO BOX 12211 RESEARCH TRIANGLE PARK NC 27709-2211
1	VERCO MATERIALS LLC R SPEYER 654 8TH STREET NW ATLANTA GA 30318

NO. OF
COPIES ORGANIZATION

1 DIRECTOR
US ARMY RSRCH LAB
RDRL D
V WEISS
ADELPHI MD 20783-1197

1 DIRECTOR
US ARMY RSRCH LAB
RDRL DP
C CHABALOWSKI
ADELPHI MD 20783-1197

ABERDEEN PROVING GROUND

61 DIR USARL
(60 HC RDRL SL
1 CD) R COATES
RDRL WM
J BAKER
S KARNA
J MCCAULEY
RDRL WML
J NEWILL (1 CD)
RDRL WML H
T FARRAND
L MAGNESS
D SCHEFFLER
R SUMMERS
RDRL WML
M ZOLTOSKI
RDRL WMM
R DOWDING
RDRL WMM A
J SANDS
RDRL WMM B
G GAZONAS
RDRL WMM D
R CARTER
E CHIN
K CHO
R SQUILLACIOTI
RDRL WMM E
M BRATCHER
J CAMPBELL
G GILDE
C HILTON
T JESSEN
S KILCZEWSKI
J LASALVIA
P PATEL
R PAVLACKA
E SHANHOLTZ

NO. OF
COPIES ORGANIZATION

A SUTORIK
J SWAB
J WRIGHT
RDRL WMM F
J MONTGOMERY
RDRL WMP
B BURNS
E SCHOENFELD
RDRL WMP B
C HOPPEL
M SCHEIDLER
T WEERASOORIYA
RDRL WMP C
T W BJERKE
J CLAYTON
D DANDEKAR
M GREENFIELD
S SEGLETES (5 CPS)
W WALTERS (5 CPS)
RDRL WMP D
T HAVEL
M KEELE
D KLEPONIS
H W MEYER
J RUNYEON
RDRL WMP E
P BARTKOWSKI
M BURKINS
W GOOCH
D HACKBARTH
E HORWATH
T JONES

NO. OF
COPIES ORGANIZATION

2 FRAUNHOFER INSTITUT FUR
KURZZEITDYNAMIK (EMI)
K THOMA
ECKERSTRASSE 4 D79 104 FREIBURG
GERMANY

1 IINDUSTREE BITOSSI SPA
R ROVAI
VIA PIETRAMARINA 53
50053 VINCI ITALY